

# NITROGEN-DOPED 9-CELL CAVITY PERFORMANCE IN THE CORNELL HORIZONTAL TEST CRYOMODULE\*

D. Gonnella<sup>†</sup>, R. Eichorn, F. Furuta, M. Ge, D. Hall, Y. He, G. Hoffstaetter, M. Liepe, T. O'Connell, S. Posen, P. Quigley, J. Sears, and V. Veshcherevich, Cornell University, Ithaca, NY, USA  
A. Grassellino and A. Romanenko, FNAL, Batavia, IL, USA

## Abstract

Cornell has recently completed construction and qualification of a horizontal cryomodule capable of holding a 9-cell ILC cavity. A nitrogen-doped niobium 9-cell cavity was assembled into the Horizontal Test Cryomodule (HTC) with a high Q input coupler and tested. We report on results from this test of a nitrogen-doped cavity in cryomodule and discuss the effects of cool down rate and thermal cycling on the residual resistance of the cavity.

## INTRODUCTION

SLAC is currently developing a superconducting CW light source, LCLS-II. In order for economic feasibility in CW operation, superconducting RF cavities in the main linac must achieve an average intrinsic quality factor ( $Q_0$ ) of  $2.7 \times 10^{10}$  at 16 MV/m and 2.0 K [1]. Nitrogen-doping of niobium cavities has been proposed to meet this high Q specification [2, 3]. In order to test the feasibility of these goals, a 1.3 GHz ILC shaped 9 cell cavity was dressed and placed in the Cornell Horizontal Test Cryomodule (HTC). The HTC has previously been used to test a 7 cell Cornell ERL cavity [4]. In this paper we discuss the results of the first nitrogen-doped 9 cell cavity tested in a cryomodule.

## METHOD

The Cornell HTC has been modified to hold a standard 9 cell ILC cavity. A schematic of the HTC with 9 cell cavity is shown in Fig. 1. The HTC accepts a cavity that is dressed with helium tank. A high Q input coupler with  $Q_L \approx 4 \times 10^{10}$  was used. The cavity was prepared with Nitrogen-doping at FNAL. It was given a bulk treatment of CBP and EP followed by a heat treatment at 800°C in vacuum for 3 hours followed by 20 minutes in 25 mTorr of nitrogen followed by an additional 30 minutes in vacuum. Finally it was given a final EP of 18 microns, dressed in a liquid helium tank at FNAL, and assembled in the cryomodule at Cornell.

Cavity performance was measured for a variety of cool downs. For each cool down,  $Q_0$  vs E was measured at 1.6, 1.7, 1.8, 1.9, 2.0, and 2.1 K. Additionally,  $Q_0$  vs E was measured for the additional TM010 modes at 2.0 K. After all of these measurements were completed, the quench field was measured at 2.0 K for all TM010 modes. For one cool down, resonance frequency vs temperature was measured during warm-up and  $Q_0$  vs temperature was measured between 1.6

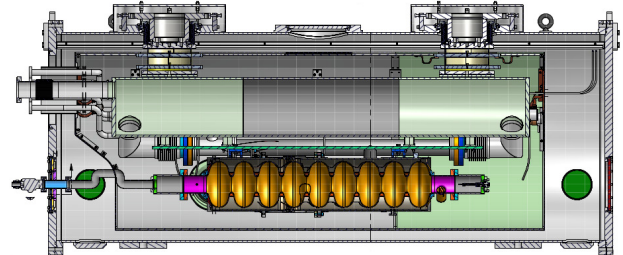


Figure 1: A schematic of the Cornell HTC with 9 cell cavity.

and 4.2 K. This data was used with SRIMP to extract material properties for the cavity [5, 6].

## COOL DOWNS AND $Q_0$ VS E PERFORMANCE

### Cool Down Dynamics

A total of four cool downs were performed (motivated by [4, 7, 8]): three fast ( $dT/dt > 1$  K/min) cool downs and one slow ( $dT/dt < 1$  K/min). The dynamics are summarized in Table 1, along with the residual resistance for each cool down.  $\frac{dT}{dt}$  is the rate of cool down near  $T_c$  and  $\Delta T_{cavity}$  is the largest temperature gradient across the cavity when it transitions from normal conducting to superconducting. Note that the  $R_{res}$  measured for the first fast cool down was after many quenches.

Table 1: Summary of Cool Down Dynamics

Cool Down	$\frac{dT}{dt}$ [K/min]	$\Delta T_{cavity}$ [K]	$R_{res}$ [n $\Omega$ ]
Fast 1	5	5	$5 \pm 1$
Fast 2	7	3	$4.0 \pm 0.8$
Slow 1	0.04	0.3	$5 \pm 1$
Fast 3	5	20	$2.7 \pm 0.5$

A profile of the fourth (fast 3) cool down is shown in Fig. 2. Temperature sensors were fixed inside the helium tank to the tops and bottoms of cells 1 and 5 and the top of cell 9. Additionally, two fluxgate magnetometers were attached to either side of cell 5, one to measure field perpendicular to the cavity axis, and one to measure field parallel to the cavity axis. From Fig. 2, we can see that below 100 K, the cavity cools from the bottom first (cells 1 and 5) followed by the tops of cells 1 and 5, while the top of cell 9 takes longer to cool. These large temperature gradients will induce thermal currents along the cavity and liquid helium tank and

\* Work supported by the US DOE and the LCLS-II Project

<sup>†</sup> dg433@cornell.edu

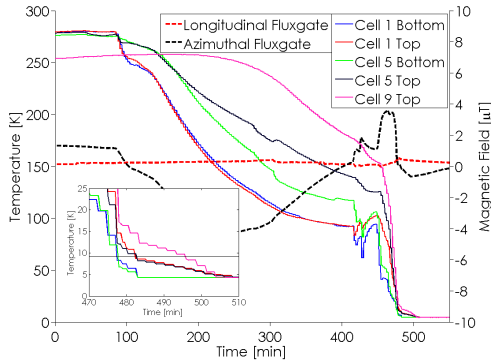


Figure 2: Temperature and magnetic field as a function of time during the fourth (fast) cool down.

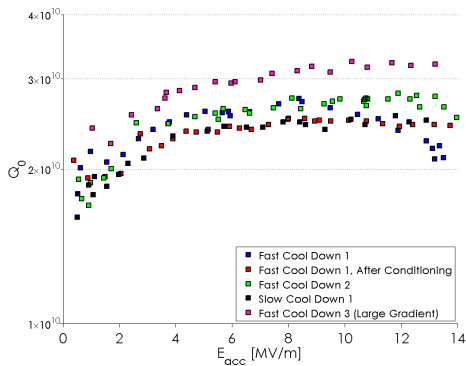


Figure 3: 2.0 K  $Q_0$  vs  $E_{acc}$  performance for all cool downs. Errors are 20% on  $Q_0$  and 10% on  $E_{acc}$ .

thus magnetic fields azimuthal to the cavity axis. Near  $T_c$  ambient fields were very small, about 2 mG, during all four cool downs so they did not impact cavity performance.

### $Q_0$ vs $E$

In all cool downs, a small anti-Q slope was observed consistent with other nitrogen-doped cavities [9]. The 2.0 K Q vs E for all four cool downs is shown in Fig. 3. For all cool downs, the cavity quenched at 14 MV/m, in agreement with the performance of the cavity in vertical test before tuning. In the first fast cool down, radiation on the order of 100 R/hr was observed at 13 MV/m, just below quench. This radiation limited the Q (to a maximum of  $2.5 \times 10^{10}$ ) but was able to be conditioned down to 100 mR/hr. This conditioning will be discussed in the next section. Following conditioning, the field emission induced Q slope above 12 MV/m was removed. The cavity was then thermally cycled to release trapped flux from cavity quenching and Q improved to a maximum of  $2.8 \times 10^{10}$ . With slow cool down, the maximum Q again dropped to  $2.5 \times 10^{10}$ . Finally, fast cool down with a large temperature gradient across the cavity during cool down resulted in the best performance:  $Q_0 = 3.2 \times 10^{10}$  at fields  $> 8$  MV/m.

From the cool down studies we can conclude that the most important parameter for high Q performance is the gradient

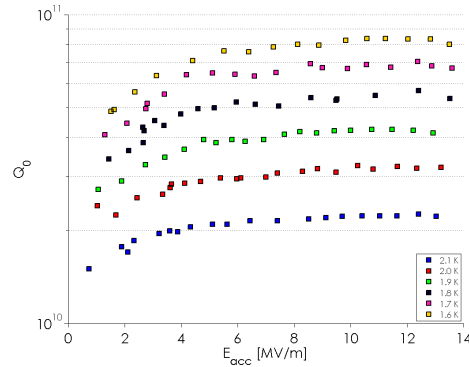


Figure 4:  $Q$  vs  $E$  at all temperatures from the fourth cool down ( $\frac{dT}{dt} = 5$  K/min,  $\Delta T = 20$  K).

across the cavity during the normal conducting to superconducting transition. We speculate that large temperature gradients facilitate the de-pinning of magnetic flux. The third fast cool down did not have the fastest cool down rate (5 K/min compared with 7 K/min in the second fast cool down) but the gradient was much larger (20 K compared with 3 K). Slow cool down resulting in lower Q is consistent with other measurements on nitrogen-doped cavities measured at Cornell and FNAL [2, 10].

Figure 4 shows the Q vs E performance of the cavity after the fourth cool down at temperatures between 1.6 and 2.1 K. At low temperature, the Q reaches as high as  $8 \times 10^{10}$ .

## CONDITIONING IN THE $8\pi/9$ MODE

During the first cool down, radiation was very high,  $\sim 100$  R/hr. By driving the cavity in the  $8\pi/9$  mode, field in the end cells is higher than in the center cells, which allows for them to reach higher fields than they could in the  $\pi$  mode. This is because the quench location is in a different cell; by keeping the field in that cell low but raising the field in the cell with the field emitter beyond 13.5 MV/m, the field emitter was able to be conditioned away. This is shown in Fig. 5, which shows the radiation as a function of maximum accelerating field for the  $8\pi/9$  mode and the  $\pi$  mode before and after conditioning. The radiation in the  $\pi$  mode is reduced by a factor of 1000 after conditioning. This demonstrates a powerful new method for conditioning field emission by driving a cavity in a different TM010 mode. This also shows that the quench field is not related to the field emitter.

## MODE MEASUREMENTS

$Q_0$  vs E for other TM010 modes were also measured at 2.0 K. From these measurement, residual resistance per cell pair (1 and 9, 2 and 8, etc.) can be extracted. These results for three of the four cool downs are shown in Fig. 6. We can see that the initial fast (small gradient) and slow cool downs resulted in a large residual resistance in cells 1 and/or 9 but this residual is reduced in the final fast cool down with large gradient over the cavity. This is most likely due to flux de-pinning in the end cells. This flux could be coming from

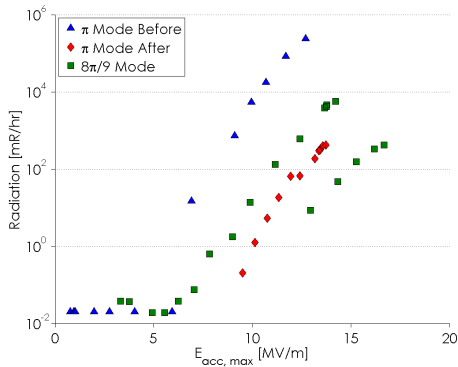


Figure 5: Field emission conditioning in the  $8\pi/9$  mode. Radiation in the  $\pi$  mode is also shown before and after conditioning.

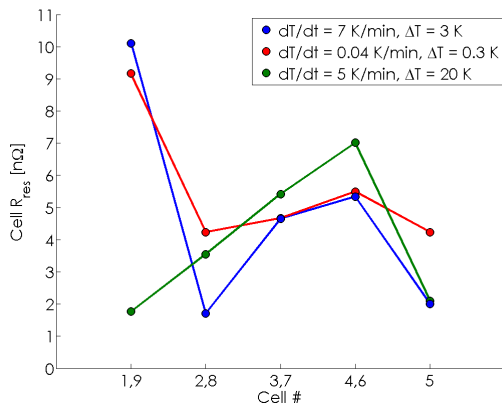


Figure 6: The residual resistance per cell pair for all cool downs. The large temperature gradient in the third fast cool down resulted in a smaller residual resistance in cells 1 and 9, likely due to reduced flux pinning from magnetic fields coming from the cavity ends.

magnetic parts in the steel beam tube sections at the cavity ends. A large temperature gradient therefore is necessary for de-pinning magnetic flux.

### MATERIAL PROPERTIES AND FIELD DEPENDENT SURFACE RESISTANCE

Material properties such as  $T_c$  mean free path, energy gap, and residual resistance can be extracted from fitting penetration depth vs temperature (obtained from resonance frequency data) and surface resistance vs temperature [11]. The extracted material properties are shown in Table 2.

Table 2: Summary of Extracted Material Properties

Property	Value
$T_c$ [K]	$9.2 \pm 0.2$
$\Delta/k_B T_c$	$1.93 \pm 0.01$
Mean Free Path [nm]	$60 \pm 20$

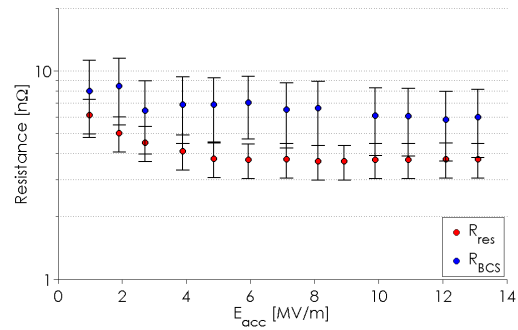


Figure 7: Deconvolution of the residual and bcs resistance as a function of accelerating field for the final fast cool down.

This fitting process can be applied to the extensive  $Q$  vs  $E$  data at temperatures between 1.6 and 2.1 K to extract residual resistance and bcs resistance as a function of accelerating field for the final fast cool down. The results of this are shown in Fig. 7. Above the low field  $Q$  slope ( $>5$  MV/m), the residual resistance is constant with increasing field. The BCS resistance drops from 8 to 6 nΩ which causes the anti- $Q$  slope between 5 and 13 MV/m. This decrease in BCS resistance is less significant than has been shown in other nitrogen-doped cavities [2], suggesting that the cavity was under-doped.

### CONCLUSIONS

Nitrogen-doping of the RF surface layer of SRF cavities has been shown to have a benefit on  $Q$  performance. We have demonstrated high  $Q$  in a nitrogen-doped 9 cell in cryomodule for the first time. The cavity achieved a  $Q$  of  $3.2 \times 10^{10}$  at 2.0 K and 13 MV/m, meeting LCLS-II  $Q_0$  specifications. The  $Q$  greatly depended on the dynamics of the cool down: a large temperature gradient during cool down is necessary to reduce pinning of ambient magnetic fields. A cool down procedure was established successfully at the Cornell HTC, which achieves the required large temperature gradients during cool down, and thus very low residual resistance in a cryomodule. We have further demonstrated using another TM010 mode to condition field emission and reduce radiation when the fundamental mode is limited by field emission or quench. These measurements are an important step on the way to demonstrating the viability of a cryomodule for LCLS-II with a  $Q$  specification of  $2.7 \times 10^{10}$  and 2.0 K and 16 MV/m.

### ACKNOWLEDGMENTS

The authors would like to thank the entire FNAL crew for preparing and dressing the cavity before shipping to Cornell. We would also like to thank the technicians at CLASSE for preparing the HTC for test.

### REFERENCES

[1] J.N. Galayda. The LCLS-II project. In *Proceedings of IPAC 2014*, Dresden, Germany, 2014.

- [2] A. Grassellino et. al. Nitrogen and argon doping of niobium for superconducting radio frequency cavities: a pathway to highly efficient accelerating structures. *Superconductor Science and Technology*, 26(102001), June 2013.
- [3] M. Liepe et. al. The joining high Q0 program for LCLS-II. In *Proceedings of IPAC 14*, Dresden, Germany, 2014.
- [4] N. Valles et. al. Cryomodule performance of the main linac prototype cavity for Cornell's energy recovery linac. In *Proceedings of NAPAC 2013*, Pasadena, CA, October 2013.
- [5] D Gonnella and M Liepe. High Q0 studies at Cornell. In *SRF 2013*, pages 475–479, 2013.
- [6] J. Halbritter. Fortran-program for the computation of the surface impedance of superconductors. *KAROLA Externer Bericht*, (3/70-6), 1970.
- [7] Julia Vogt, Oliver Kugeler, Jens Knobloch, and Helmholtz-zentrum Berlin. Quest for High Q0: residual Resistance Elimination. In *SRF 2013*, September 2013.
- [8] A Romanenko, A Grassellino, O Melnychuk, and D A Ser-gatskov. Dependence of the residual surface resistance of SRF cavities on the cooling rate through Tc. *ArXiv*, pages 1–6, 2014.
- [9] D. Gonnella et. al. New insights into heat treatment of srf cavities in a low pressure nitrogen atmosphere. In *Proceedings of IPAC 14*, Dresden, Germany, 2014.
- [10] D. Gonnella et. al. Flux trapping in nitrogen doped and 120c baked cavities. In *Proceedings of IPAC 14*, Dresden, Germany, 2014.
- [11] Dan Gonnella and Matthias Liepe. Heat treatment of srf cavities in a low-pressure nitrogen atmosphere. In *Proceedings of SRF 13*, Paris, France, September 2013.